01 Jan 2009

An Improved UPFC Control for Oscillation Damping

Jagannathan Sarangapani
Missouri University of Science and Technology, sarangap@mst.edu

Mariesa Crow
Missouri University of Science and Technology, crow@mst.edu

Jianjun Guo

Recommended Citation

J. Sarangapani et al., "An Improved UPFC Control for Oscillation Damping," *IEEE Tranactions on Power Systems*, vol. 24, no. 1, pp. 288-296, Institute of Electrical and Electronics Engineers (IEEE), Jan 2009. The definitive version is available at https://doi.org/10.1109/TPWRS.2008.2008676

An Improved UPFC Control for Oscillation Damping

J. Guo, *Student Member, IEEE*, M. L. Crow, *Senior Member, IEEE*, and Jagannathan Sarangapani, *Senior Member, IEEE*

***Abstract*—This paper proposes a new control approach for a unified power flow controller (UPFC) for power system oscillation damping. This control is simple to implement, yet is valid over a wide range of operating conditions. It is also effective in the presence of multiple modes of oscillation. The proposed control is implemented in several test systems and is compared against a traditional PI control.**

***Index Terms*—Oscillation damping, power system stability, unified power flow controller (UPFC).**

I. Introduction

ONE of the most promising network controllers for the bulk power system is the family of power electronics-based controllers, known as "flexible ac transmission system" (FACTS) devices. FACTS devices work by modifying power flow in individual lines of the power grid, maintaining voltage stability, and damping oscillations. The DOE National Transmission Grid Study released in May 2002 identified FACTS devices as playing a significant role in the "Intelligent Energy System" of the future. This rapid control has been shown to be effective in achieving voltage support and stability improvement, thus allowing the transmission system to be operated more efficiently with a smaller stability margin. The rapid development of the power electronics industry has made FACTS devices increasingly attractive for utility deployment due to their flexibility and ability to effectively control power system dynamics. The primary function of the FACTS is to control the transmission line power flow; the secondary functions of the FACTS can be voltage control, transient stability improvement and oscillation damping. The unified power flow controller (UPFC) is the most versatile FACTS device. The UPFC is able to simultaneously provide both series and shunt compensation to a transmission line providing separate control of the active and reactive powers on the transmission line.

In recent years, the use of the UPFC for oscillation damping has received increased attention. Several approaches have been taken to the modeling and control of the UPFC. Perhaps the most common approach is to model the UPFC as a power injection model [1]–[3]. The power injection model neglects the dynamics of the UPFC and uses the UPFC active and reactive power injection as the control inputs into the power system. This approach has the advantages of simplicity and computational efficiency since the fast dynamics of the UPFC are neglected.

Manuscript received November 07, 2006; revised July 29, 2008. First published January 09,2009; current version published January 21, 2009. Paper no. TPWRS-00782-2006.

The authors are with the Electrical and Computer Engineering Department, Missouri University of Science and Technology, Rolla, MO 65409-0810 USA.

Digital Object Identifier 10.1109/TPWRS.2008.2008676

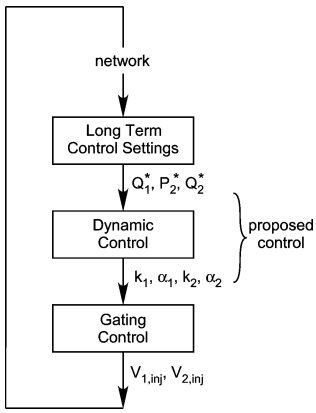

Fig. 1. UPFC hierarchical control.

While effective from a high-level control viewpoint, this approach assumes that the UPFC is ideally (and instantaneously) able to provide the required active and reactive powers.

In the cases where UPFC dynamics are included, the most common approach to controlling the UPFC has been to use PI control [4]–[7]. PI control is simple to implement, yet very effective in damping an oscillatory mode when it is properly tuned. PI control is less effective in damping oscillations that contain multiple modes. For multiple mode damping, several lead-lag blocks are required that require additional coordinated tuning. Secondly, PI control becomes increasingly less effective as the system conditions move from the operating point around which the controller was tuned. For this reason, it is desirable to develop controllers that are impervious to changes in operating condition and that are effective for multiple mode oscillation damping. In this paper, a new control is proposed that is effective over a wider range of operating conditions and is able to damp multiple modes effective. Specifically in this paper, we will

1) present the development of a new control for the UPFC;
2) show its effectiveness over a range of operating conditions and multiple modes; and
3) compare it with a traditional PI control method.

The proposed control is the dynamic control required to achieve given active and reactive power flow and voltage setpoints. All system level control tacitly assumes that the UPFC can instantaneously achieve the required setpoints. However, there can be degradation of performance if a significant time lag exists between the time the setpoint is given and the time at which the UPFC achieves the desired injected voltages. The proposed controller is a nonlinear dynamic control that translates the desired system level control into gating control as shown in Fig. 1.

Ideally, the system level control setpoints would not be constant powerflows (or current injections), but rather would be

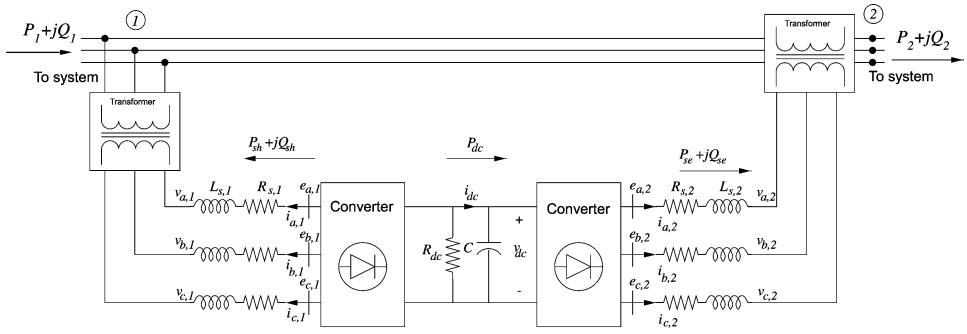

Fig. 2. Unified power flow controller diagram.

time varying in order to achieve the desired system response (i.e., oscillation damping). This paper asserts that a linear control (such as the PI control) is inadequate to track a moving target due to the requirement that it be tuned for different operating conditions and requires a much larger number of parameters. The proposed nonlinear control has the advantages of rapid tracking and is independent of tuning.

II. UPFC State Model

The unified power flow controller, or UPFC, is the most versatile FACTS device. It consists of a combination of a shunt and series branches connected through the dc capacitor as shown in Fig. 2. The series connected inverter injects a voltage with controllable magnitude and phase angle in series with the transmission line, therefore providing real and reactive power to the transmission line. The shunt-connected inverter provides the real power drawn by the series branch and the losses and can independently provide reactive compensation to the system. The UPFC model is a combination of the synchronous static compensator (STATCOM) and static series synchronous compensator (SSSC) models [8] as follows:

$$\frac{1}{\omega_s}\frac{d}{dt}i_{d_1} = \frac{k_1 V_{dc}}{L_{s_1}}\cos(\alpha_1+\theta_1) + \frac{\omega}{\omega_s}i_{q_1} - \frac{R_{s_1}}{L_{s_1}}i_{d_1} - \frac{V_1}{L_{s_1}}\cos\theta_1 \tag{1}$$

$$\frac{1}{\omega_s}\frac{d}{dt}i_{q_1} = \frac{k_1 V_{dc}}{L_{s_1}}\sin(\alpha_1+\theta_1) - \frac{R_{s_1}}{L_{s_1}}i_{q_1} - \frac{\omega}{\omega_s}i_{d_1} - \frac{V_1}{L_{s_1}}\sin\theta_1 \tag{2}$$

$$\frac{1}{\omega_s}\frac{d}{dt}i_{d_2} = -\frac{R_{s_2}}{L_{s_2}}i_{d_2} + \frac{\omega}{\omega_s}i_{q_2} + \frac{k_2}{L_{s_2}}\cos(\alpha_2+\theta_1)V_{dc} - \frac{1}{L_{s_2}}(V_2\cos\theta_2 - V_1\cos\theta_1) \tag{3}$$

$$\frac{1}{\omega_s}\frac{d}{dt}i_{q_2} = -\frac{R_{s_2}}{L_{s_2}}i_{q_2} - \frac{\omega}{\omega_s}i_{d_2} + \frac{k_2}{L_{s_2}}\sin(\alpha_2+\theta_1)V_{dc} - \frac{1}{L_{s_2}}(V_2\sin\theta_2 - V_1\sin\theta_2) \tag{4}$$

$$\frac{C}{\omega_s}\frac{d}{dt}V_{dc} = -k_1\cos(\alpha_1+\theta_1)i_{d_1} - k_1\sin(\alpha_1+\theta_1)i_{q_1} - k_2\cos(\alpha_2+\theta_1)i_{d_2} - k_2\sin(\alpha_2+\theta_1)i_{q_2} - \frac{V_{dc}}{R_{dc}} \tag{5}$$

where the parameters are as shown in Fig. 2. The currents i_{d1} and i_{q1} are the dq components of the shunt current. The currents i_{d2} and i_{q2} are the dq components of the series current. The voltages $V_1\angle\theta_1$ and $V_2\angle\theta_2$ are the shunt and series voltage magnitudes and angles, respectively. The UPFC is controlled by varying the phase angles (α_1, α_2) and magnitudes (k_1, k_2) of the converter shunt and series output voltages (e_1, e_2), respectively.

The power balance equations at bus 1 are given by

$$0 = V_1\left((i_{d_1}-i_{d_2})\cos\theta_1 + (i_{q_1}-i_{q_2})\sin\theta_1\right) - V_1\sum_{j=1}^{n} V_j Y_{1j}\cos(\theta_1-\theta_j-\phi_{1j}) \tag{6}$$

$$0 = V_1\left((i_{d_1}-i_{d_2})\sin\theta_1 - (i_{q_1}-i_{q_2})\cos\theta_1\right) - V_1\sum_{j=1}^{n} V_j Y_{1j}\sin(\theta_1-\theta_j-\phi_{1j}) \tag{7}$$

and at bus 2

$$0 = V_2\left(i_{d_2}\cos\theta_2 + i_{q_2}\sin\theta_2\right) - V_2\sum_{j=1}^{n} V_j Y_{2j}\cos(\theta_2-\theta_j-\phi_{2j}) \tag{8}$$

$$0 = V_2\left(i_{d_2}\sin\theta_2 - i_{q_2}\cos\theta_2\right) - V_2\sum_{j=1}^{n} V_j Y_{2j}\sin(\theta_2-\theta_j-\phi_{2j}). \tag{9}$$

From the figure, the following quantities are defined:

P_1, Q_1	powers injected from the system into bus 1;
P_2, Q_2	powers injected from bus 2 into the system;
P_{sh}, Q_{sh}	powers injected by the shunt converter;
P_{se}, Q_{se}	powers injected by the series converter;

P_{dc} active power from shunt to series converter less losses;

$P_{\text{inj}}, Q_{\text{inj}}$ powers injected by the series transformer $= V_{\text{inj}} I_2^*$ where $V_{\text{inj}} = V_1 - V_2$.

III. New UPFC Control

A. Series Control

The control objective for the series portion of the UPFC is inject a variable series voltage into the line such that the line powers track a desired active line power $P_2^\star$ and desired reactive power $Q_2^\star$. The target values are chosen for the particular power system application and may be chosen to be a constant value or to damp oscillations. In addition, the shunt portion of the UPFC is utilized to maintain the bus voltage at the sending end (bus 1 in Fig. 2) and the dc link capacitor voltage. The inputs α_1, k_1, α_2, and k_2 are controlled to achieve these objectives.

Starting with the series portion of the UPFC, the desired powers are converted into desired currents $i_{d_2}^\star$ and $i_{q_2}^\star$ through

$$\begin{bmatrix} i_{d_2}^\star \\ i_{q_2}^\star \end{bmatrix} = \begin{bmatrix} \cos\theta_2 & \sin\theta_2 \\ \sin\theta_2 & -\cos\theta_2 \end{bmatrix}^{-1} \begin{bmatrix} P_2^\star/V_2 \\ Q_2^\star/V_2 \end{bmatrix}. \tag{10}$$

Note that in per unit, the current in both windings of the series transformer are the same value, therefore the desired line power flows are used to calculate the target series currents.

To track the target, new state variables e_{d_2} and e_{q_2} are defined such that

$$e_{d_2} = i_{d_2}^\star - i_{d_2} \tag{11}$$
$$e_{q_2} = i_{q_2}^\star - i_{q_2} \tag{12}$$

leading to new state equations

$$\begin{aligned} \frac{d}{dt}e_{d_2} &= \frac{d}{dt}i_{d_2}^\star + \frac{\omega_s R_{s_2}}{L_{s_2}} i_{d_2} \\ &\quad - \omega i_{q_2} - \frac{\omega_s k_2}{L_{s_2}} \cos(\alpha_2 + \theta_1) V_{dc} \\ &\quad + \frac{\omega_s}{L_{s_2}} (V_2 \cos\theta_2 - V_1 \cos\theta_1) \end{aligned} \tag{13}$$

$$\begin{aligned} \frac{d}{dt}e_{q_2} &= \frac{d}{dt}i_{q_2}^\star + \frac{\omega_s R_{s_2}}{L_{s_2}} i_{q_2} \\ &\quad + \omega i_{d_2} - \frac{\omega_s k_2}{L_{s_2}} \sin(\alpha_2 + \theta_1) V_{dc} \\ &\quad + \frac{\omega_s}{L_{s_2}} (V_2 \sin\theta_2 - V_1 \sin\theta_1). \end{aligned} \tag{14}$$

Let control inputs be defined as

$$u_{21} = k_2 \cos\alpha_2 \tag{15}$$
$$u_{22} = k_2 \sin\alpha_2. \tag{16}$$

A positive definite Lyapunov function is given by

$$V = \frac{c}{2} e_{d_2}^2 + \frac{c}{2} e_{q_2}^2, c > 0. \tag{17}$$

The derivative of V is given by

$$\dot{V} = p_1 u_{21} + p_2 u_{22} + p_3 - c \frac{R_{s_2}\omega_s}{L_{s_2}} \left(e_{d_2}^2 + e_{q_2}^2\right) \tag{18}$$

where

$$\begin{aligned} p_1 &= -c \frac{\omega_s}{L_{s_2}} V_{dc} \left(e_{d_2} \cos\theta_1 + e_{q_2} \sin\theta_1\right) \\ p_2 &= c \frac{\omega_s}{L_{s_2}} V_{dc} \left(e_{d_2} \sin\theta_1 - e_{q_2} \cos\theta_1\right) \\ p_3 &= c \left(e_{d_2} \frac{d}{dt} i_{d_2}^\star + e_{q_2} \frac{d}{dt} i_{q_2}^\star \right) \\ &\quad + c \frac{R_{s_2}\omega_s}{L_{s_2}} \left(e_{d_2} i_{d_2}^\star + e_{q_2} i_{q_2}^\star\right) \\ &\quad - c\omega \left(e_{d_2} i_{q_2}^\star - e_{q_2} i_{d_2}^\star\right) \\ &\quad + c \frac{\omega_s}{L_{s_2}} \left(e_{q_2} (V_2 \sin\theta_2 - V_1 \sin\theta_1) \right. \\ &\quad \left. + e_{d_2} (V_2 \cos\theta_2 - V_1 \cos\theta_1)\right). \end{aligned}$$

The derivative $\dot{V}$ is guaranteed to be negative if

$$p_1 u_{21} + p_2 u_{22} + p_3 = -c_2 \left(e_{d_2}^2 + e_{q_2}^2\right), c_2 > 0. \tag{19}$$

Therefore from Lyapunov's second theorem on stability [9], this system is asymptotically stable if (19) is satisfied provided the control inputs are selected as

$$\begin{bmatrix} u_{21} \\ u_{22} \end{bmatrix} = C_2^{-1} \left\{ E_2 - \begin{bmatrix} \omega_s \frac{R_{s_2}}{L_{s_2}} - c_2 & -\omega_s \\ \omega_s & \omega_s \frac{R_{s_2}}{L_{s_2}} - c_2 \end{bmatrix} \begin{bmatrix} e_{d_2} \\ e_{q_2} \end{bmatrix} \right\} \tag{20}$$

where

$$C_2 = \frac{\omega_s V_{dc}}{L_{s_2}} \begin{bmatrix} \cos\theta_1 & -\sin\theta_1 \\ \sin\theta_1 & \cos\theta_1 \end{bmatrix}$$

$$E_2 = \begin{bmatrix} \frac{\omega_s}{L_{s_2}} \left(R_{s_2} i_{d_2} + V_2 \cos\theta_2 - V_1 \cos\theta_1\right) - \omega i_{q_2} + \frac{d}{dt} i_{d_2}^\star \\ \frac{\omega_s}{L_{s_2}} \left(R_{s_2} i_{q_2} + V_2 \sin\theta_2 - V_1 \sin\theta_1\right) + \omega i_{d_2} + \frac{d}{dt} i_{q_2}^\star \end{bmatrix}.$$

Equations (15) and (16) can be solved for k_2 and α_2 from

$$k_2 = \sqrt{u_{21}^2 + u_{22}^2} \tag{21}$$

and

$$\alpha_2 = \begin{cases} \tan^{-1} \frac{u_{22}}{u_{21}} & u_{21} > 0 \\ \tan^{-1} \frac{u_{22}}{u_{21}} + \pi & u_{21} < 0 \\ \sin^{-1} \frac{u_{22}}{k_2} & u_{21} = 0. \end{cases} \tag{22}$$

Both k_2 and α_2 are limited to bound the magnitude of the injected current and therefore limit the injected active and reactive powers. The parameter c_2 is usually chosen to be a large number and may be tuned to obtain the desired damping time frame.

A finer control may be achieved however, by introducing an additional parameter such that (20) becomes

$$C_2\begin{bmatrix}u_{21}\\u_{22}\end{bmatrix}=E_2-\begin{bmatrix}\omega_s\frac{R_{s_2}}{L_{s_2}}-c_2 & -\omega_s\\ \omega_s & \omega_s\frac{R_{s_2}}{L_{s_2}}-c_2\end{bmatrix}\begin{bmatrix}e_{d_2}\\e_{q_2}\end{bmatrix}. \tag{23}$$

By splitting c_2 into two separate parameters (c_{d_2} and c_{q_2}), a weighted control is possible whereby i_{d_2} or i_{q_2} can be more tightly controlled, and subsequently P_2 or Q_2.

B. Shunt Control

The control objective for the shunt portion of the UPFC is two-fold. The first objective is to regulate the shunt bus voltage magnitude at the reference value. This is similar to the voltage control aspect of a STATCOM. The second objective is to maintain the dc link capacitor voltage. The control of many voltage sourced converters (such as the STATCOM and SSSC) requires a near constant dc link voltage to have effective control. While the dc link capacitor may discharge briefly during transients to provide active power to the system, a significant voltage sag may result in severe control degradation as the converter is no longer able to inject the desired current into the system.

The voltage magnitude at the shunt bus is primarily impacted by injected reactive power, whereas the dc link voltage is primarily impacted by the active power absorbed by the shunt converter to charge the capacitor. Therefore a similar control approach for the STATCOM can be derived such that

$$\begin{bmatrix}i^\star_{d_2}-i^\star_{d_1}\\ i^\star_{q_2}-i^\star_{q_1}\end{bmatrix}=\begin{bmatrix}\cos\theta_1 & \sin\theta_1\\ \sin\theta_1 & -\cos\theta_1\end{bmatrix}^{-1}\begin{bmatrix}P^\star_1/V_1\\ Q^\star_1/V_1\end{bmatrix}. \tag{24}$$

The desired reactive power $Q^\star_{sh}$ is the reactive power required for voltage support at the shunt bus and may be chosen independently. The desired active power $P^\star_{sh}$ however is not independent of $P^\star_{se}$. The shunt active power must account for the losses in the shunt and series branches of the UPFC and is therefore

$$P^\star_1=-(P^\star_{se}+P_{\text{loss}}) \tag{25}$$

where

$$P_{\text{loss}}=R_{s_2}\left(i^2_{d_2}+i^2_{q_2}\right)+R_{s_1}\left(i^2_{d_1}+i^2_{q_1}\right)+\frac{V^2_{dc}}{R_{dc}}. \tag{26}$$

It is not possible to *a priori* designate an exact target value for P_{loss}, but a target value can be estimated. From the series control, values for $i^\star_{d_2}$ and $i^\star_{q_2}$ can be obtained. One objective of the shunt portion is to maintain V_{dc} at a constant value, thus $V^\star_{dc}$ can also be specified. Thus

$$\begin{aligned}P^\star_{\text{loss}}&=R_{s_2}\left(\left(i^\star_{d_2}\right)^2+\left(i^\star_{q_2}\right)^2\right)\\&\quad+R_{s_1}\left(\left(i^\star_{d_1}\right)^2+\left(i^\star_{q_1}\right)^2\right)\\&\quad+\frac{(V^\star_{dc})^2}{R_{dc}}+k(V^\star_{dc}-V_{dc}).\end{aligned} \tag{27}$$

The last term in (27) reflects the dependence of P_{loss} on V_{dc}. The constant k is a nonnegative number. Substituting these values into (24) yields

$$\begin{aligned}&\cos\theta_1\left(i^\star_{d_2}-i^\star_{d_1}\right)+\sin\theta_1\left(i^\star_{q_2}-i^\star_{q_1}\right)\\&\quad=\Bigg(P^\star_{se}+R_{s_1}\left(\left(i^\star_{d_1}\right)^2+\left(i^\star_{q_1}\right)^2\right)\\&\qquad+R_{s_2}((i^\star_{d_2})^2+(i^\star_{q_2})^2)\\&\qquad+\frac{(V^\star_{dc})^2}{R_{dc}}+k\left(V^\star_{dc}-V_{dc}\right)\Bigg)/V_1\end{aligned} \tag{28}$$

$$\sin\theta_1\left(i^\star_{d_2}-i^\star_{d_1}\right)-\cos\theta_1\left(i^\star_{q_2}-i^\star_{q_1}\right)=Q^\star_1/V_1. \tag{29}$$

These equations can then be solved for $i^\star_{d_1}$ and $i^\star_{q_1}$. Since these equations are nonlinear, to have an exact solution for $i^\star_{d_1}$ and $i^\star_{q_1}$ requires the iterative solution of (28) and (29). In most cases however, a fairly close approximation can be obtained by solving

$$\begin{aligned}\begin{bmatrix}i^\star_{d_1}\\ i^\star_{q_1}\end{bmatrix}&=-\frac{1}{V_1}\begin{bmatrix}\cos\theta_1+2i^0_{d_1}\frac{R_{s_1}}{V_1} & \sin\theta_1+2i^0_{q_1}\frac{R_{s_1}}{V_1}\\ \sin\theta_1 & -\cos\theta_1\end{bmatrix}^{-1}\\&\times\begin{bmatrix}P^\star_2+R_{s_2}\left(\left(i^\star_{d_2}\right)^2+\left(i^\star_{q_2}\right)^2\right)+\frac{(V^\star_{dc})^2}{R_{dc}}+k(V^\star_{dc}-V_{dc})\\ Q^\star_1\end{bmatrix}\end{aligned}$$

where $i^0_{d_1}$ and $i^0_{q_1}$ are the initial shunt current values.

Following the same procedure above, new state variables e_{d_1} and e_{q_1} are defined

$$e_{d_1}=i^\star_{d_1}-i_{d_1} \tag{30}$$

$$e_{q_1}=i^\star_{q_1}-i_{q_1} \tag{31}$$

and

$$\begin{aligned}\begin{bmatrix}u_{11}\\u_{12}\end{bmatrix}=C_1^{-1}\Bigg\{&E_1-\\&\begin{bmatrix}\omega_s\frac{R_{s_1}}{L_{s_1}}-c_1 & -\omega_s\\ \omega_s & \omega_s\frac{R_{s_1}}{L_{s_1}}-c_1\end{bmatrix}\begin{bmatrix}e_{d_1}\\e_{q_1}\end{bmatrix}\Bigg\}\end{aligned} \tag{32}$$

where

$$C_1=\frac{\omega_s V_{dc}}{L_{s_1}}\begin{bmatrix}\cos\theta_1 & -\sin\theta_1\\ \sin\theta_1 & \cos\theta_1\end{bmatrix}$$

$$E_1=\begin{bmatrix}\frac{\omega_s}{L_{s_1}}(R_{s_1}i^\star_{d_1}+V_1\cos\theta_1)-\omega i^\star_{q_1}+\frac{d}{dt}i^\star_{d_1}\\ \frac{\omega_s}{L_{s_1}}(R_{s_1}i^\star_{q_1}+V_1\sin\theta_1)+\omega i^\star_{d_1}+\frac{d}{dt}i^\star_{q_1}\end{bmatrix}$$

and

$$u_{11}=k_1\cos\alpha_1$$

$$u_{12}=k_1\sin\alpha_1$$

from which k_1 and α_1 can be determined similar to (21) and (22).

IV. Control Implementation

The series and shunt controls proposed in the previous section are first applied to the small test system shown in Fig. 3. This system is a two-area system with one low frequency interarea mode in the 1.0-Hz range. Bus 11 is a virtual bus added to the

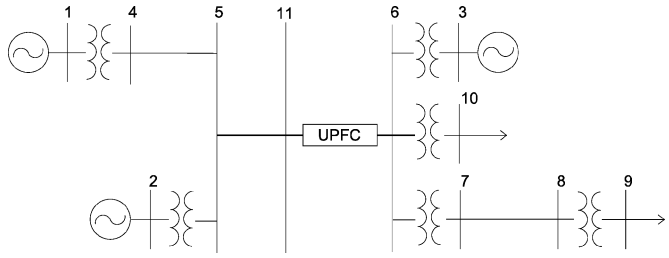

Fig. 3. Two-area test system.

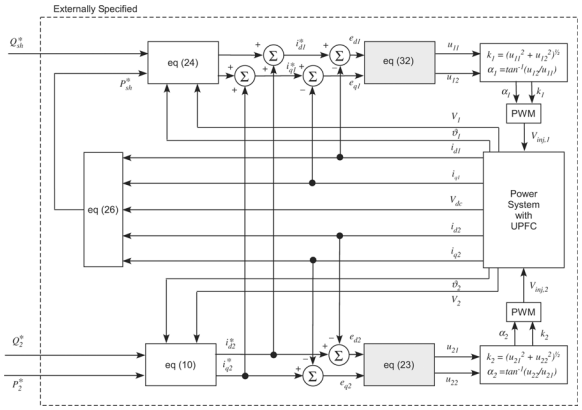

Fig. 4. Control framework.

system. The generators are modeled as two-axis generators with a simple dc exciter, voltage regulator, and turbine/governor. The generator and network equations are given in the Appendix.

The primary objective of the UPFC is to damp the resulting interarea oscillations. Additional objectives are to maintain the dc link capacitor voltage V_{dc} and the voltage at bus 6. The proposed controller is compared against a PI controller where

$$\begin{bmatrix} u_{11} \\ u_{12} \end{bmatrix} = \begin{bmatrix} K_{1dd} & K_{1dq} \\ K_{1qd} & K_{1qq} \end{bmatrix} \begin{bmatrix} e_{d1} \\ e_{q1} \end{bmatrix} + \begin{bmatrix} K_{1ddI} & K_{1dqI} \\ K_{1qdI} & K_{1qqI} \end{bmatrix} \int \begin{bmatrix} e_{d1} \\ e_{q1} \end{bmatrix} \tag{33}$$

$$\begin{bmatrix} u_{21} \\ u_{22} \end{bmatrix} = \begin{bmatrix} K_{2dd} & K_{2dq} \\ K_{2qd} & K_{2qq} \end{bmatrix} \begin{bmatrix} e_{d2} \\ e_{q2} \end{bmatrix} + \begin{bmatrix} K_{2ddI} & K_{2dqI} \\ K_{2qdI} & K_{2qqI} \end{bmatrix} \int \begin{bmatrix} e_{d2} \\ e_{q2} \end{bmatrix}. \tag{34}$$

The PI parameters were initially chosen via standard procedures [10] and then further refined using a genetic algorithm to produce the best results possible [11].

For an even comparison, both the PI controller and the proposed controller are based on the same control scheme shown in Fig. 4. This control is based on dq series and shunt current injections as determined by (10) and (24). Fig. 4 shows the control diagram for the controllers. The only difference between the proposed controller and the PI controller is the shaded blocks, in which (23) is replaced by (33) and (32) is replaced by (34). However, note that the PI controller requires 16 parameters whereas the proposed controller has three parameters (c_1, c_2, k). The parameters for the proposed control are chosen to be large positive constants and require very little tuning. The parameters for both controllers are given in Tables I and II for Cases I and II.

TABLE I
PROPOSED CONTROLLER PARAMETERS

c_d	1000
c_q	1000
k	10

TABLE II
PI CONTROLLER PARAMETERS FOR CASES I AND II

K_{1dd}	-6.86e-03	K_{2dd}	1.21e-01
K_{1dq}	-2.98e-01	K_{2dq}	-7.72e-05
K_{1qd}	5.43e-02	K_{2qd}	-3.51e-03
K_{1qq}	3.89e-02	K_{2qq}	-4.16e-01
K_{1ddI}	2.34e-01	K_{2ddI}	-9.67e-02
K_{1dqI}	1.26e-02	K_{2dqI}	-9.28e-04
K_{1qdI}	2.59e-02	K_{2qdI}	-1.46e-01
K_{1qqI}	1.96e-02	K_{2qqI}	-8.00e-00

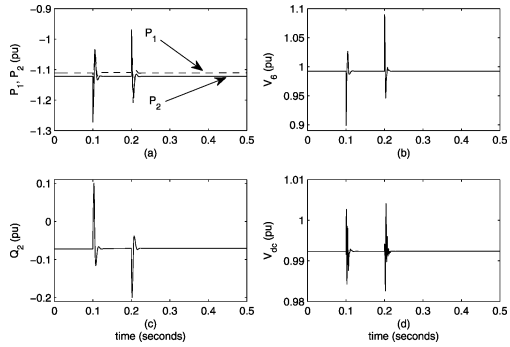

Fig. 5. UPFC control values—Case I.

It is possible to neglect the cross-coupling terms in the PI controller ($K_{1dq}, K_{1qd}, K_{2dq}$, etc.) to yield only eight parameters that need to be tuned. There is a slight degradation in performance when these mutual affect terms are neglected.

A. Case I

At 0.1 s, a three-phase-to-ground fault is applied to the system on bus 10. The fault is cleared at 0.2 s without removing any lines. The UPFC is designed to control four quantities to a reference value: P_2, Q_2, V_1 and V_{dc}. These results are summarized in Fig. 5 for constant reference values. The active power P_1 is also shown in Fig. 5(a). Note that since P_2 and Q_2 are constant, bus 5 simulates a constant "PQ" bus, thus the fault on bus 10 does not sufficiently propagate into area 1. Since the active and reactive power at bus 5 only varies slightly, generators 1 and 2 only experience slight variations due to intra-area oscillations, but the interarea oscillations are substantially reduced. These are shown (along with ω_3) in Fig. 6. Similarly, bus 6 is essentially a "PV" bus with constant power (P_1) and voltage (V_6) and area 1 and area 2 are essentially decoupled by the UPFC.

The system dynamics responses compared against the PI controller and no control are shown in Figs. 7–10 for the parameters given in Tables I and II. In Figs. 7–9 the dotted lines indicate the uncontrolled system dynamic responses. The system is stable but exhibits sustained interarea oscillations. The response of the system with the PI controller is shown with the thin line. The proposed controller response is the bold line. Fig. 7 shows the active power flow on the tie line between areas 1 and 2. Both controllers exhibit good damping response as compared to the

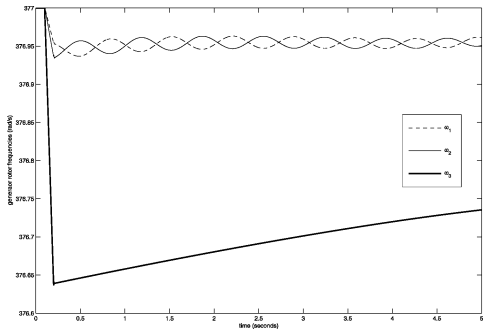

Fig. 6. Generator frequencies (rad/s)—proposed control—Case I.

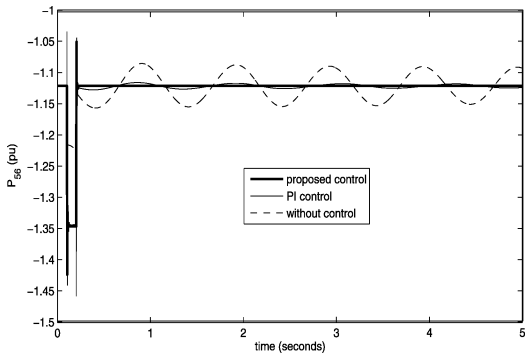

Fig. 7. Active power between buses 5 and 6—Case I.

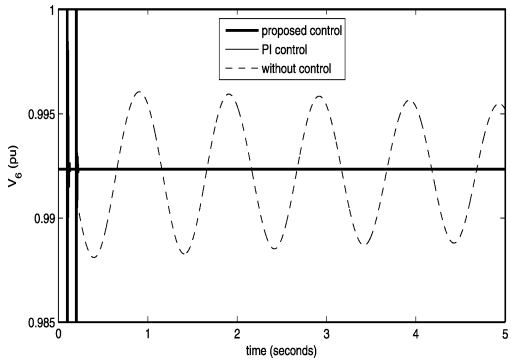

Fig. 8. Voltage magnitude at bus 6—Case I.

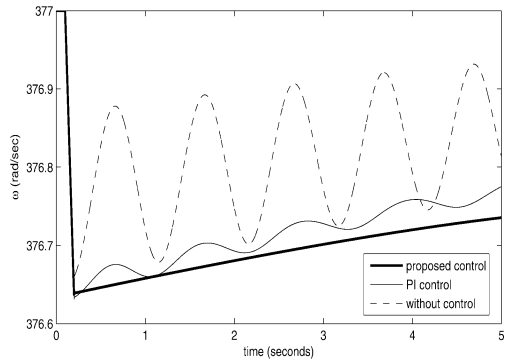

Fig. 9. Generator frequencies—Case I.

undamped case. Fig. 8 shows the voltage at bus 6. The results of the PI and proposed controller are virtually indistinguishable and both show excellent voltage control. Fig. 9 shows the frequency dynamics of generator 3. Both controllers show similar damping as compared to the uncontrolled case.

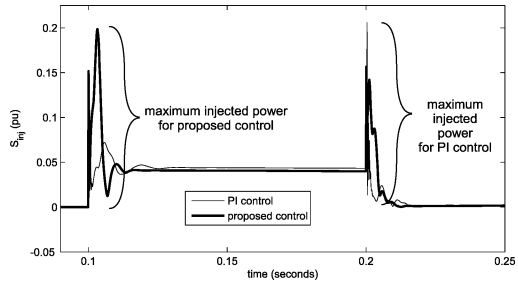

Fig. 10. Injected UPFC power for PI and proposed control—Case I.

Fig. 10 shows the injected power during the fault which is less than 20% of the steady-state power flow on the line. Note that the power injection for the proposed control is greatest at the fault initiation (0.1 s), whereas the PI control is maximum at the fault clearing (0.2 s). During the fault (after transients), the power injection of both controllers is nearly the same. This similar behavior allows an even comparison between controllers. Both controllers exhibit a "spike" at fault initiation and clearing. This is due to the slight time delay before the controller reacts. This is an artifact of the transmission model used—the algebraic network equations provide instantaneous propagation of the fault behavior throughout the system. In actuality, the fault propagation rate depends on the dynamics of the RLC transmission network and is not instantaneous—therefore in practical situations, the spike magnitude would probably not be as high. The duration of the spike depends on several factors: the controller design, the sampling rate of the digital signal processor, the switching frequency of the power electronics, and the microprocessor speed. In the results shown, the only factor apparent is the controller design and the "sampling rate" which can be considered to be the time step length of the time domain simulation. In this case, both controllers can be said to act equally fast.

B. Case II

One substantial difference between linear and nonlinear controllers is that linearized control is typically optimized around a single operating point, but a nonlinear controller is relatively independent of a particular operating point. To illustrate the differences in controller response, the same controllers (same parameters) are now subjected different operating conditions. In this case, the same system is used except that the generator inertias are altered slightly to change the frequency of the interarea mode. the power flow response to the same disturbance is shown in Fig. 11. The uncontrolled system is stable with sustained oscillations. The proposed controller still exhibits good damping characteristics with very rapid damping. The PI controller still damps the oscillations but at a much slower rate. To be effective, the PI controller must be retuned to the new frequency of oscillation.

C. Case III

In this section, the effectiveness of the proposed control is studied for a more severe fault—one in which the UPFC injected

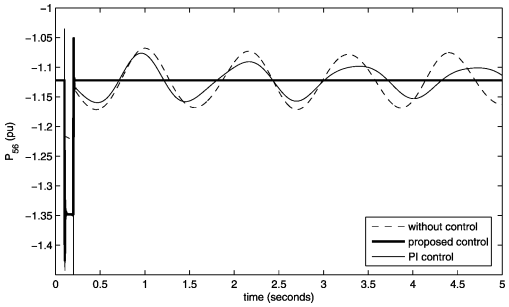

Fig. 11. Active power between buses 5 and 6—Case II.

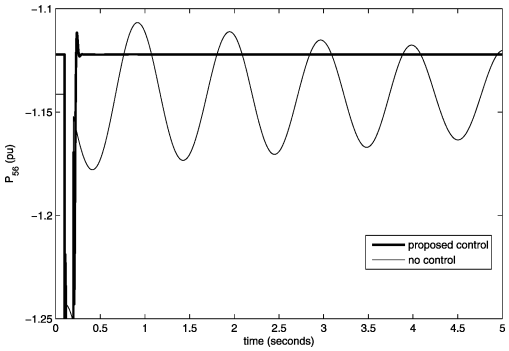

Fig. 12. Active power between buses 5 and 6—Case III.

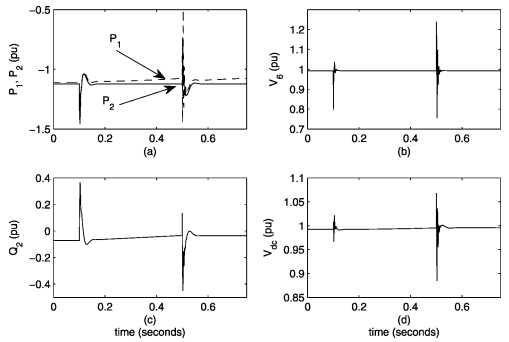

Fig. 13. UPFC control values—Case III.

power exceeds its limits. In this case, the fault is not removed until 0.5 s. The resulting active power flow on line 5–6 is shown in Fig. 12 has roughly twice the swing magnitude of Case I. Similar to Fig. 5, all of the controlled parameters are shown in Fig. 13.

However, the injected power exceeds 20% of the steady-state power flow on the line (assumed to be the UPFC limit). Therefore, constraints are put on the injected power to keep it below the UPFC limit. The injected power under limited and non-limited operation are shown in Fig. 14. The dashed line indicates the maximum injected power limit. The resulting active power flows on line 5–6 are shown in Fig. 15. Note that although the performance of the UPFC in maintaining a constant active power on the line is somewhat degraded, it rapidly brings the power flow back to the reference once the fault is cleared.

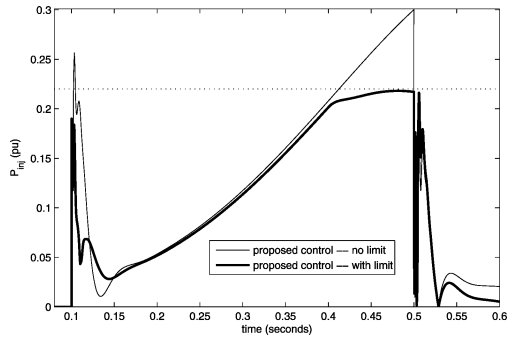

Fig. 14. UPFC injected power—Case III.

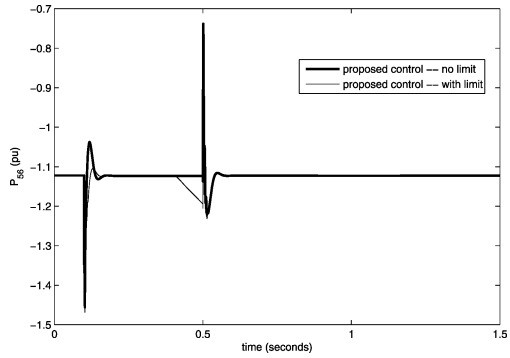

Fig. 15. Active power between buses 5 and 6—Case III.

D. Case IV

Next, the proposed controller's effectiveness was tested in the 118 bus test system shown in Fig. 16. The UPFC was placed on line 26–30 and a three-phase-to-ground fault occurred on bus 43 at 0.2 s and was cleared at 0.4 s. The UPFC objective was to regulate the post fault active power flow on the line. Without the controller, highly nonlinear active power oscillations are induced by the fault as shown in Fig. 17. As in the small test system, the proposed controller exhibits near immediate control.

Fig. 18 shows the injected power from the UPFC required to achieve the damping shown in Fig. 17. Note that the amount of injected active power is considerably less than the amount of active power flow on the line and is only a few percent of the line rating.

E. Case V

In the last case, two UPFCs are placed in the 118 bus system. They are placed on lines 5–11 (at bus 5) and 7–12 (at bus 7). These placements were chosen such that the two UPFCs were in close proximity to see if they adversely affected each other's performance. In this case, the reference values of each UPFC's powers were altered such that (SS indicates steady-state):

These values were chosen to show the impact of both positive and negative reference values on the behavior of the UPFCs. The dynamic impact of these changes are shown in Figs. 19–21. Fig. 19 shows all of the series and shunt powers of the two UPFCs in response to the commanded reference changes. The top plot shows the active series powers of the UPFCs. UPFC1 is shown as the solid trace whereas UPFC2 is the dashed trace. The middle plot shows the series reactive powers and the bottom plot

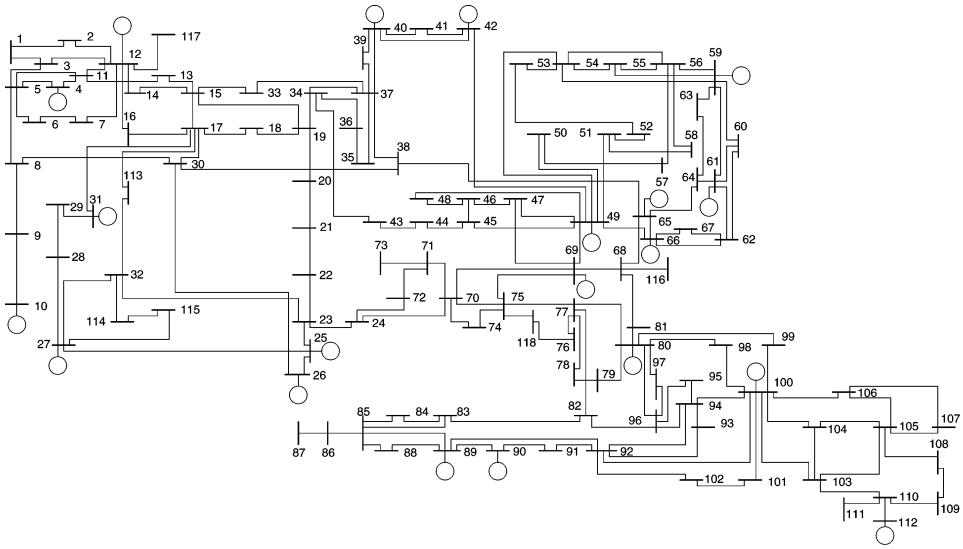

Fig. 16. IEEE 118-bus test system.

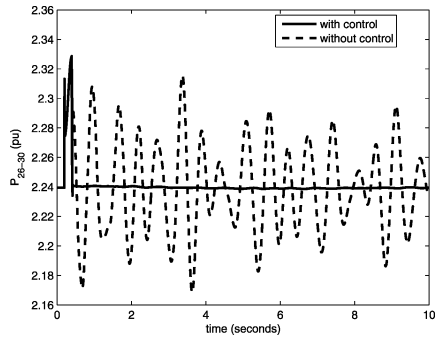

Fig. 17. Active power between buses 26 and 30—Case IV.

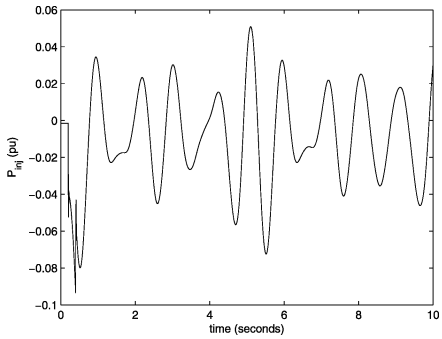

Fig. 18. UPFC injected active power—Case IV.

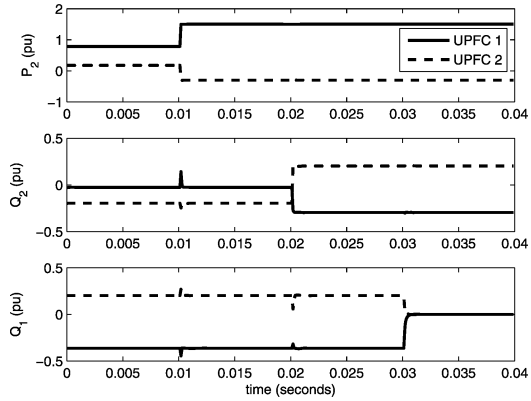

Fig. 19. Active and reactive UPFC powers—Case V.

	UPFC 1 (5-11)			UPFC 2 (7-12)		
	$P_2^\star$	$Q_2^\star$	$Q_1^\star$	$P_2^\star$	$Q_2^\star$	$Q_1^\star$
$0 \le t \le 0.1$	SS	SS	SS	SS	SS	SS
$0.1 < t \le 0.2$	1.5	–	–	-0.3	–	–
$0.2 < t \le 0.3$	–	-0.3	–	–	0.2	–
$0.3 < t \le 0.4$	–	–	0.0	–	–	0.0

shows the shunt injected reactive power. The active power references are commanded to change at 0.1 s. Note that the active powers respond rapidly to the change in commanded powers. There is a slight impact on both the series and shunt reactive powers, but they rapidly return to their commanded values. The series reactive power is commanded to change at 0.2 s. As expected, this change has more impact on the shunt injected reactive power than on the series active power, but once again, the shunt reactive power returns to the commanded value rapidly. Lastly, the shunt reactive power is commanded to change at 0.3 s. This change has little impact on the series active and reactive powers.

Fig. 20 shows the dc link capacitor voltage of the two UPFCs throughout the changes. Note that aside from brief small transients at the time of reference changes, the dc link capacitor voltages remain constant. This indicates good stability of the control and ensures good performance of the UPFC.

Fig. 21 shows the bus voltage magnitudes at either end of the transmission line on which the two UPFCs are placed. The voltages behave as expected in response to the changes in the active and reactive powers.

These results indicate that the proposed control enables independent control of the three independent UPFC attributes (series active power, series reactive power, and shunt reactive power). The shunt active power depends on the charge and discharge of the dc link capacitor and the UPFC losses.

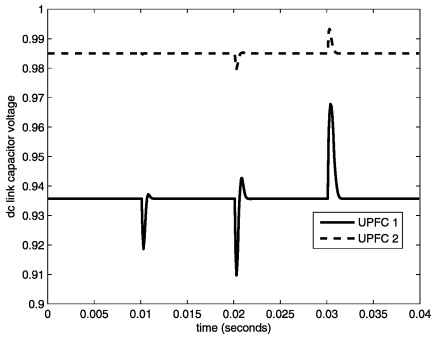

Fig. 20. DC link capacitor voltages—Case V.

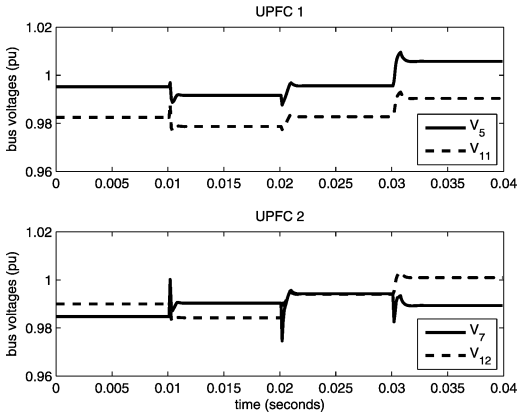

Fig. 21. Bus voltages—Case V.

V. Conclusion

In this paper, a new control for the UPFC was proposed. The proposed control exhibited very good performance in damping active power oscillations and maintaining the UPFC shunt bus voltage. It exhibited favorable performance when compared with a PI controller under several operating conditions. The proposed control works well in both large and small systems with rapid dynamic response and independent control. The primary advantages of the proposed control are 1) it works over a wide range of operating conditions, 2) requires only three parameters, and 3) the parameters are easily chosen and do not require considerable tuning effort.

References

[1] B. Chaudhuri, B. C. Pal, A. Zolotas, I. Jaimoukha, and T. Green, "Mixed-sensitivity approach to H_∞ control of power system oscillations employing multiple FACTS devices," *IEEE Trans. Power Syst.*, vol. 18, no. 3, pp. 1149–1156, Aug 2003.

[2] M. M. Farsangi, Y. H. Song, and K. Y. Lee, "Choice of FACTS device control inputs for damping interarea oscillations," *IEEE Trans. Power Syst.*, vol. 19, no. 2, pp. 1135–1143, May 2004.

[3] B. C. Pal, "Robust damping of interarea oscillations with unified power-flow controller," *Proc. Inst. Elect. Eng. Gen., Transm., Distrib.*, vol. 149, no. 6, pp. 733–738, Nov. 2002.

[4] E. Gholipour and S. Saadate, "Improving of transient stability of power systems using UPFC," *IEEE Trans. Power Del.*, vol. 20, no. 2, pp. 1677–1682, Apr. 2005.

[5] S. Kannan, S. Jayaram, and M. Salama, "Real and reactive power coordination for a unified power flow controller," *IEEE Trans. Power Syst.*, vol. 19, no. 3, pp. 1454–1461, Aug. 2004.

[6] N. Tambey and M. L. Kothari, "Damping of power system oscillations with unified power flow controller (UPFC)," *Proc. Inst. Elect. Eng. Gen., Transm., Distrib.*, vol. 150, no. 2, pp. 129–140, Mar. 2003.

[7] H. Wang, "A Unified model for the analysis of FACTS devices in damping power system oscillations—Part III: Unified power flow controller," *IEEE Trans. Power Del.*, vol. 15, no. 3, pp. 978–983, Jul. 2000.

[8] L. Dong, M. L. Crow, Z. Yang, and S. Atcitty, "A reconfigurable FACTS system for university laboratories," *IEEE Trans. Power Syst.*, vol. 19, no. 1, pp. 120–128, Feb. 2004.

[9] H. K. Khalil, *Nonlinear Systems*. Upper Saddle River, NJ: Prentice-Hall, 2002.

[10] S. Skogestad and I. Postlethwaite, *Multivariable Feedback Control: Analysis and Design*. West Sussex, NJ: Wiley, 1996.

[11] A. Bomfim, G. Taranto, and D. Falcao, "Simultaneous tuning of power system damping controllers using genetic algorithms," *IEEE Trans. Power Syst.*, vol. 15, no. 1, pp. 163–169, Feb. 2000.

J. Guo (S'03) received the B.S. degree from Nanchang University in 1995, the M.S. degree from Harbin Engineering University, Harbin, China, in 2001, and the Ph.D. degree from the University of Missouri-Rolla in 2006.

He is currently employed by Operation Technology, Inc. (ETAP). He is interested in robust control and power system dynamics.

M. L. Crow (SM'94) received the B.S.E. degree from the University of Michigan at Ann Arbor in 1985 and the Ph.D. degree in 1989 from the University of Illinois at Urbana-Champaign.

Currently, she is the Dean for the School of Materials, Energy, and Earth Resources and a Professor in the Department of Electrical and Computer Engineering at the University of Missouri-Rolla. Her research interests include developing computational methods for dynamic security assessment and the application of power electronics in bulk power systems.

Jagannathan Sarangapani (SM'99) received the Ph.D. degree from the University of Texas at Arlington in 1994.

Currently, he is a Professor in the Department of Electrical and Computer Engineering at the University of Missouri-Rolla. His research interests include adaptive control and neural network control, control of networks, and embedded systems.